# Influence of a dc offset field on kicked quasi-one-dimensional Rydberg atoms: Stabilization and frustrated field ionization

S. Yoshida,[1] C. O. Reinhold,[2,3] J. Burgdörfer,[1,3] W. Zhao,[4] J. J. Mestayer,[4] J. C. Lancaster,[4] and F. B. Dunning[4]
[1]*Institute for Theoretical Physics, Vienna University of Technology, Vienna, Austria*
[2]*Physics Division, Oak Ridge National Laboratory, Oak Ridge, Tennessee 37831-6372, USA*
[3]*Department of Physics, University of Tennessee, Knoxville, Tennessee 37996, USA*
[4]*Department of Physics and Astronomy and the Rice Quantum Institute, Rice University, Houston, Texas 77005-1892, USA*
(Received 2 December 2005; published 8 March 2006)

The influence of a superposed offset field on the response of highly polarized (quasi-1D) very-high-$n$ Rydberg atoms to a periodic train of unidirectional half-cycle pulses (HCPs) is investigated, both experimentally and theoretically. It is observed that the presence of an offset field strongly influences the dynamics. The electronic states become transiently stabilized and trapped near the ionization threshold when the net average field they experience is near zero irrespective of whether the HCPs, applied parallel to the atomic axis, are directed towards or away from the nucleus. The nature of this stabilization is explored using Poincaré surfaces of section. In large offset fields, direct field ionization becomes possible but it is demonstrated that this can be suppressed by application of an oppositely directed HCP train. The use of such "frustrated field ionization" to measure the polarization of Rydberg atoms is discussed.

DOI: 10.1103/PhysRevA.73.033411 PACS number(s): 32.80.Rm, 32.80.Qk, 32.60.+i

## I. INTRODUCTION

Simple periodically-driven systems can provide valuable insights into the correspondence between classical and quantum dynamics. This is particularly true for systems that exhibit classical chaos because in this case [1–3] quantum dynamics tends to differ significantly from its classical counterpart. One manifestation of this is quantum localization where the quantum wave function becomes localized while the classical phase space density shows chaotic diffusion. In contrast, when a system undergoes periodic or quasiperiodic motion, the corresponding quantum wave functions mimic their classical counterparts. The quantum wave function stabilizes around the periodic classical trajectories and becomes localized without dispersion [4–6]. It has recently been suggested [7–10] that such localization around the classical periodic motion can be used to control and manipulate wave packets. Thus, not only are simple periodically driven systems used as a theoretical testing ground to study classical-quantum correspondence but also their realization may lead to various applications in atomic engineering.

The periodically kicked Rydberg atom provides an example of such a driven system that has now been realized experimentally. When a Rydberg atom is subject to a pulsed unidirectional electric field, termed a half-cycle pulse (HCP), whose duration $T_p$ is much shorter than the classical electron orbital period $T_n$, the HCP simply delivers an impulsive momentum transfer or "kick"

$$\Delta p = -\int_0^\infty F^{\mathrm{HCP}}(t)dt \tag{1}$$

to the Rydberg electron, where $F^{\mathrm{HCP}}(t)$ is the field produced by the HCP (atomic units are used throughout). The application of a train of identical HCPs equispaced in time with interval $T_T$, described by

$$F_{\mathrm{train}}(t) = \sum_{k=0}^{N-1} F^{\mathrm{HCP}}(t - kT_T) \tag{2}$$

can lead to dynamical stabilization, the Rydberg electron undergoing (classical) periodic motion that is synchronized with the train. The resulting electronic wave packets have been observed experimentally [11,12] as peaks in the survival probability as the pulse repetition frequency $\nu_T(=1/T_T)$ is varied.

The impulsive limit $T_p \ll T_n$ can be reached using very-high-$n$ Rydberg atoms ($n \sim 350$) and nanosecond-duration HCPs produced by applying output pulses from a fast pulse generator to a nearby electrode. Much shorter subpicosecond HCPs can be produced using photoconducting switches that are triggered by femtosecond laser pulses [13–16] allowing studies at intermediate $n$, $n \sim 30$. Recently it has been suggested that it might even be feasible to produce trains of attosecond-duration HCPs by appropriately combining harmonics generated through high harmonic conversion using a two-color laser field [17].

A fundamental difference exists between HCPs produced by photoconducting switches or high harmonic generation and those produced by pulse generators. The former ultrashort pulses represent freely propagating electromagnetic waves. As such, the solution of Maxwell's equations requires that the vector potential at the conclusion of the pulse vanish, i.e.,

$$A(t=\infty) = -c\int_{-\infty}^{\infty} F(t)dt = 0 \tag{3}$$

or, generally, the net momentum transfer to a free electron [Eq. (1)] must vanish [18]. This, however, does not preclude the possibility of achieving significant momentum transfer to an electron in an atom because the atom responds nonlin-

 

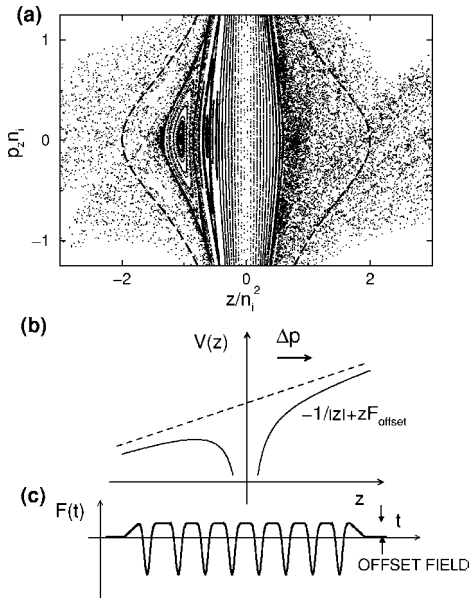


FIG. 1. (a) Poincaré surface of section for a train of HCPs delivering scaled impulses $\Delta p_0=0.24$ with scaled frequency $\nu_0=\nu_T/\nu_{n_i}=2.7$, and an offset field $F_{\text{offset}}=\Delta p/T_T$ (see text). The surface of section is taken for $(\rho,p_\rho)\sim(0,0)$ and is classically scale invariant under a variation of $n_i$. The dashed lines show the initial energy manifold for a state of energy $-1/(2n_i^2)$. (b) Potential distribution in the presence of the offset field. (c) Time dependence of the field $F(t)=F_{\text{offset}}(t)+F^{\text{HCP}}(t)$.

early to strong external fields due to the presence of the Coulomb field. For such electrons it is the large field amplitude near the peak of the HCPs that is important, rather than the integral over the entire temporal field distribution.

For a train of $N$ unipolar HCPs, the momentum transfer to a free electron is given by $\Delta p_{\text{free}}=N\Delta p$ and is equivalent to that produced by a constant field

$$\bar{F}_{\text{HCP}}=-\frac{\Delta p_{\text{free}}}{NT_T}=-\frac{\Delta p}{T_T} \tag{4}$$

over the same time interval $NT_T$. By applying an offset field $F_{\text{offset}}$ during the HCP train the net external field experienced by the electrons can be varied and will be zero when

$$F_{\text{offset}}=-\bar{F}_{\text{HCP}}=\frac{\Delta p}{T_T}. \tag{5}$$

In this case the behavior of a Rydberg atom in the combined field should mirror that in a freely propagating electromagnetic field [Eq. (3)]. The presence of the offset field can dramatically modify the dynamical response of the atom to the HCP train.

In the present paper we investigate the dynamics of highly elongated quasi-one-dimensional (quasi-1D) Rydberg atoms in the combined presence of an offset field $F_{\text{offset}}$ and a train of HCPs, i.e., in the field $F(t)$

$$F(t)=F_{\text{offset}}(t)+F_{\text{train}}(t) \tag{6}$$

shown in Fig. 1(c). We focus on two aspects: the dependence of the dynamics on the polarization of the Rydberg state relative to the applied fields, and the suppression of static field ionization by a sequence of HCPs, referred to in the following as "pulse-frustrated field ionization" which shows that application of HCPs can lead to bound-state survival rather than ionization.

Both behaviors depend strongly on the average field experienced by the atom, this being especially evident when the time integral over the total field $F(t)$ [Eq. (6)] vanishes. Here we investigate this regime through both experiment and classical trajectory Monte Carlo (CTMC) simulations. In the case of small fields, i.e., small kicks ($\Delta p_0=n\Delta p\ll 1$), enhanced stability is seen irrespective of the orientation of the initial polarized state. Pulse-frustrated field ionization is observed for larger fields ($\Delta p_0\lesssim 1$) when the offset field becomes sufficiently strong to classically field ionize the atoms. We show that pulse-frustrated field ionization can provide a measure of the degree of initial polarization (i.e., elongation) of quasi-1D Rydberg states.

## II. EXPERIMENT

The present apparatus is described in more detail elsewhere [11,19,20]. Briefly, quasi-1D high-$n$ atoms are created by photoexciting, in a weak dc field of $\sim$300 $\mu$Vcm$^{-1}$, potassium atoms contained in a thermal-energy beam to selected low-lying redshifted $n=350$, $m=0$ Stark states using an extra-cavity doubled CR699-21 Rh6G dye laser. Experiments are conducted in a pulsed mode. The laser output is formed into a train of pulses of $\sim$1 $\mu$s duration and $\sim$20 kHz repetition frequency using an acousto-optic modulator. (The probability that a Rydberg atom is formed during any laser pulse is small and data must be accumulated following many laser pulses.) Immediately following each laser pulse the atoms are subject to the train of HCPs and superposed offset field that is generated by applying voltage pulses to a nearby electrode. The overall applied waveform is measured using a fast probe and sampling oscilloscope. The number of surviving Rydberg atoms is determined using selective field ionization (SFI). For this, a slowly varying positive voltage ramp is applied to the lower interaction region electrode. Electrons resulting from field ionization are accelerated to, and detected by, a particle multiplier. Measurements in which no HCPs or offset field are applied are interspersed at routine intervals during data acquisition to monitor the number of Rydberg atoms initially created. The Rydberg atom survival probability is then determined by taking the ratio of the Rydberg atom signals observed with and without application of the pulsed fields.

## III. THEORETICAL METHODS

The experimental results are analyzed using CTMC simulations. The (restricted) microcanonical ensemble of points in phase space that represents the initial mix of Stark states (taken as a distribution of 36 Stark states centered on the parabolic quantum number $n_1=320$ [20]) is propagated in time according to Hamilton's equation of motion for the Hamiltonian

$$H(t) = H_{\rm at} + V(t) \tag{7}$$

with

$$H_{\rm at} = \frac{p^2}{2} - \frac{1}{r}, \quad V(t) = zF(t), \tag{8}$$

where $\vec{r}=(x,y,z)$ and $\vec{p}=(p_x,p_y,p_z)$ are the position and momentum of the electron, respectively. Calculations using a $K^+$ core ion potential showed that the use of a simple hydrogenic Coulomb potential does not significantly influence the theoretical predictions. The final energy $E_f$ of the electron is determined at the end of the propagation time, i.e., at the end of pulse train. The overall survival probability is then given by the fraction of the initial conditions for which $E_f<0$. In practice, product states with very large values of $n$ above some cut off $n_{\rm max}$ are field ionized as a result of field inhomogeneities present in the apparatus. Tests suggest that this cutoff lies in the range $800 \lesssim n_{\rm max} \lesssim 1000$ and calculations are presented for both of these values. Moreover, the sequence of HCPs is not perfectly periodic with small random variations occurring in both the time interval $T_T$ between the pulses and in their amplitude. We therefore include both amplitude and frequency noise in our simulations to check for the effects of nonperiodic driving on stabilization.

We consider in the following the modifications to the ionization dynamics produced by the presence of an offset field that is (typically) turned on just before the HCP train and turned off just after it ends. We assume that the kicks are applied in the positive $z$ direction ($\Delta p>0$) [see Figs. 1(b) and 1(c)]. Accordingly, the average HCP field $\bar{F}_{\rm HCP}$ [Eq. (4)] is oriented in the negative $z$ direction. When the condition in Eq. (5) is satisfied, the offset field $F_{\rm offset}$ is pointing in the $+z$ direction and the combined field

$$F_{\rm av} = F_{\rm offset} + \bar{F}_{\rm HCP} = F_{\rm offset} - \Delta p/T_T \tag{9}$$

vanishes.

In order to explore the stability properties when $F_{\rm av} \simeq 0$ we employ Poincaré surfaces of section. Figure 1(a) displays one such section for a scaled kick strength $\Delta p_0=0.24$, a scaled frequency $\nu_0=\nu_T/\nu_n=2.7$, ($\nu_n=1/T_n$), and an offset field such that $F_{\rm av}=0$. It is assumed that the HCP train is perfectly periodic and that the HCP train and offset field continue indefinitely. The figure corresponds to stroboscopic snapshots taken at those times when the field associated with successive HCPs is at a maximum. Given that the present atoms are quasi-1D, surfaces of section are taken at $(\rho,p_\rho) \equiv [\sqrt{x^2+y^2},(xp_x+yp_y)/\rho] \sim (0,0)$. Since the kicks are directed in the $+z$ direction, electrons with $z<0 (>0)$ experience kicks towards (away from) the nucleus. Figure 1 therefore allows the behavior under both these driving conditions to be examined.

Even though the phase space for a 1D atom subject to kicks directed away from the nucleus, corresponding to the ($z>0$) part of the Poincaré section, is known to be globally chaotic [21] Fig. 1(a) exhibits quasistable structures near the nucleus ($z=0$) (the nearly parallel straight lines to the right of the origin). These are due to the finite width of the HCPs and disappear in the limit of ultrashort HCPs. For kicks directed towards the nucleus, i.e., the $z<0$ region of the Poincaré section, quasiregular elongated islands are observed, which are related to stable KAM tori seen in the 1D system. For the present 3D system, however, we find that these structures are a manifestation of cantori, i.e., remnants of broken KAM tori. (Similar behavior has been observed for Rydberg atoms subject to a periodic train of kicks that alternate in sign [12,22].) No tori or cantori are visible in Fig. 1 in regions of phase space that overlap the initial high Rydberg states, represented by the classical tori indicated by the dashed lines in Fig. 1(a). Rather, these states lie entirely in the chaotic sea. The enhanced stability of high Rydberg states when $F_{\rm av}=0$ analyzed below is therefore due to the slowing down of chaotic diffusion rather than to the appearance of stable islands. The phase space structure of Fig. 1 immediately implies that the stabilization will be transient but robust against noise. Were quasistable islands responsible for the enhanced survival these would be destroyed by noise leading to a pronounced drop in the survival probability.

## IV. STABILIZATION FOR WEAK KICKS: DIRECTIONAL INDEPENDENCE

The survival probability for quasi-1D $n_i=350$ Rydberg atoms polarized along the $+z$ axis and subject to $N=20$ HCPs that provide kicks in the $+z$ direction, i.e., away from the nucleus, is shown in Fig. 2 as a function of the time-averaged field $F_{\rm av}$ for several scaled frequencies $\nu_0$. Each HCP has a full width at half maximum (FWHM) duration of $\sim$600 picoseconds and delivers a scaled momentum transfer $\Delta p_0=n_i\Delta p=0.24$. The survival probability depends markedly on the net time-averaged field peaking near $F_{\rm av}\sim 0$ for all scaled frequencies $\nu_0$. Figure 2 also includes the results of CTMC simulations. These show that the enhanced stability near $F_{\rm av}\sim 0$ is insensitive to the presence of noise in the form of random fluctuations in HCP period and amplitude of up to $\pm 5\%$, consistent with the fact that the initial tori reside in the chaotic sea. Furthermore, the result is only weakly dependent on the precise value of the cutoff quantum number (energy) $n_{\rm max}$. The overall agreement between the experimental data and the simulations is quite good.

The enhanced stability can be understood in terms of directed chaotic diffusion from the initial bound states ($E<0$) towards the ionization threshold. As the mean $n$ increases the atomic momentum $p_n=1/n$ characterizing the motion in the Coulomb field of the nucleus (or, equivalently, the Compton profile) becomes small compared to the kick

$$p_n \ll \Delta p \tag{10}$$

or in terms of scaled momentum $p_{n,0}=n_i/n$, $p_{n,0} \ll \Delta p_0$. In this limit, the electron behaves as a quasifree particle and suffers no net momentum transfer. The offset field itself may be viewed as delivering a series of impulsive kicks to the excited electron that are in the opposite direction to those delivered by the HCPs. When these are of equal magnitude, i.e., when $F_{\rm av}=0$, the effect of the impulse delivered by each HCP is, in essence, immediately canceled by the impulse from the offset field. On average, therefore, the motion of the electron is little perturbed by the pulse train and little net

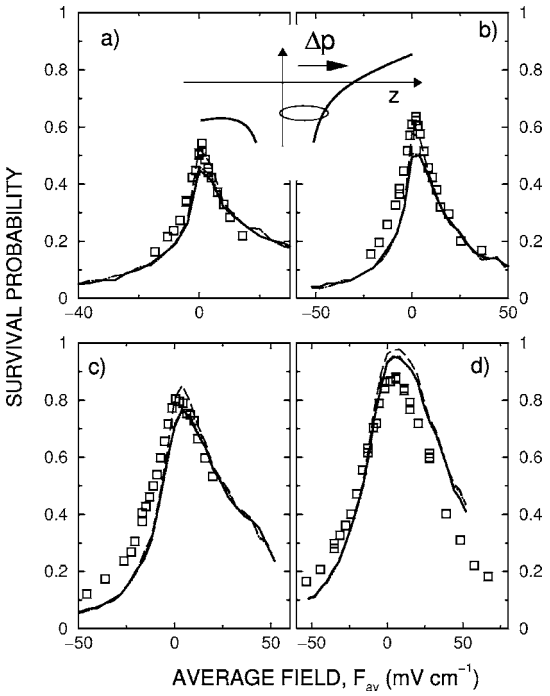


FIG. 2. Survival probabilities for quasi-1D $n_i=350$ Rydberg atoms subject to $N=20$ HCPs as a function of net average field $F_{\mathrm{av}}$. The initial quasi-1D state is polarized along the $+z$ axis, parallel to the impulses delivered by the HCPs (see inset) which are of scaled magnitude $\Delta p_0=n_i\Delta p=0.24$. The scaled frequencies of the HCPs are (a) 0.33, (b) 0.5, (c) 1.3, and (d) 2.7. The open squares are experimental data, the lines the results of CTMC simulations for (---) $n_{\max}=1000$, (·····) $n_{\max}=800$, and (—) $n_{\max}=800$ with ±5% noise included (see text).

transfer of energy or momentum to it occurs.

The quasifree limit can also be viewed as the limit of high scaled frequencies. Although the initial scaled frequencies $\nu_0=\nu_T/\nu_{n_i}$ that can be realized in the present experiments are limited to values $\leqslant 3$, the first HCPs in the train rapidly move the distribution of electron binding energies towards higher energies, i.e., larger values of $n$. Because the classical electron orbital frequency decreases rapidly with $n$, $\nu_n \propto n^{-3}$, the electron enters a regime where the effective scaled frequency of the HCPs, $\nu_0'=\nu_T/\nu_n$ becomes very large. This slows diffusion to the continuum and the electron energy distribution becomes transiently localized and trapped near the continuum. This is illustrated in Fig. 3 which shows the electron energy distribution in scaled units $E_0=n_i^2E$ for quasi-1D $n_i=350$ atoms following application of a train of $N=20$ HCPs with scaled frequencies $\nu_0=0.33$ and 2.7. Each HCP delivers a scaled impulse $\Delta p_0=0.24$ and the offset field is chosen such that $F_{\mathrm{av}}=0$. The electron energy distributions are strongly peaked near $E=0$. Interestingly, the peak in the electron energy distributions shifts towards higher energies, i.e., higher $n$, as $\nu_0$ decreases. This results because the values of $n$ at which the high frequency limit is realized increase as $\nu_0$ decreases.

Since the tori representing initial states oriented in either the positive ($z>0$) or negative ($z<0$) direction, i.e., uphill or downhill Stark states in the offset field, both lie in the

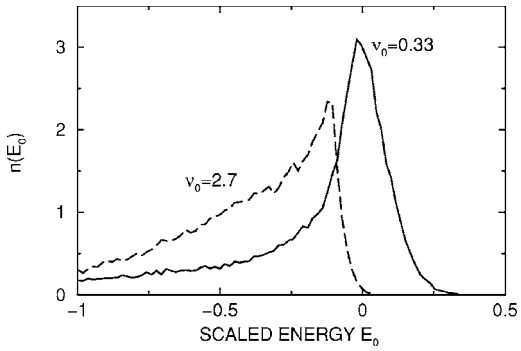


FIG. 3. Electron energy distributions for quasi-1D $n_i=350$ Rydberg atoms subject to $N=20$ HCPs when $F_{\mathrm{av}}=0$. Each HCP delivers a scaled impulse $\Delta p_0=0.24$ at scaled frequencies of (—) $\nu_0=0.33$ and (----) $\nu_0=2.7$. 5% noise is included. The electron energy is expressed in scaled units $E_0=n_i^2E$. The initial state is polarized along the $+z$ axis.

chaotic sea, similar transient stabilization is to be expected for both initial polarizations. This is, indeed, the case as demonstrated by Fig. 4 which shows the survival probability for quasi-1D $n_i=350$ atoms polarized along the $-z$ axis following application of $N=20$ kicks ($\Delta p_0=0.24$) in the $+z$ direction, i.e., directed towards the nucleus, as a function of the time averaged field $F_{\mathrm{av}}$ [Eq. (9)] for the same scaled frequencies $\nu_0$, values of $n_{\max}$, and noise as in Fig. 2. The calculated survival probabilities are in good agreement with the experimental data. A sharp peak in survival probability is seen near $F_{\mathrm{av}}=0$ which, simulations show, is again associated with trapping of the electron energy distribution near the continuum. The present results therefore indicate that the survival probability is governed primarily by the size of the

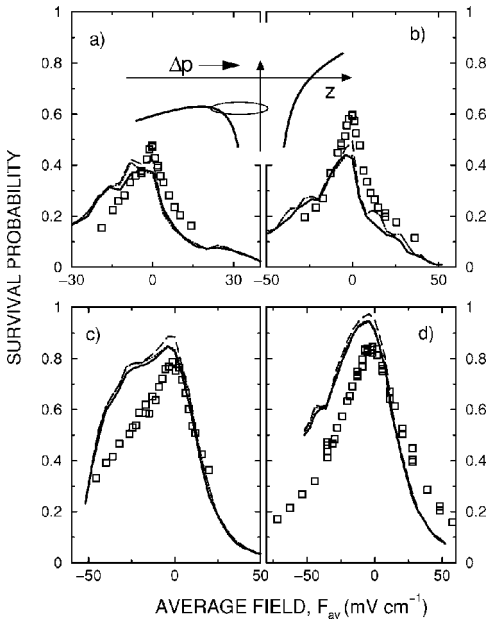


FIG. 4. Survival probabilities for quasi-1D $n_i=350$ Rydberg atoms subject to $N=20$ HCPs as a function of the net average field $F_{\mathrm{av}}$. The initial state is polarized along the $-z$ axis, antiparallel to the impulses delivered by the HCPs (see inset). The scaled frequencies $\nu_0$ and the scaled impulses $\Delta p_0$ are as in Fig. 2.

average field $F_{\rm av}$ rather than by the initial orientation of the atom.

The universality of the enhanced transient stabilization near threshold when $\nu_T \gg \nu_n$ or $\Delta p_{n,0} \ll \Delta p_0$ can be analytically verified. For $\nu_T \gg \nu_n$ the high-frequency limit is reached, i.e., $T_T \ll T_n = 2\pi n^3$. Stabilization requires that the total energy transfer $\Delta E$ due to both $\bar{F}_{\rm HCP}$ and $F_{\rm offset}$ vanishes to first order in $T_T$. Considering one period of the train extending from a half period $(T_T/2)$ before the kick to a half period after it, the energy transfer by a kick $\Delta p$ (in the impulsive limit for simplicity) is

$$\Delta E^{\rm kick} \simeq \frac{(p_z+\Delta p)^2}{2} - \frac{p_z^2}{2} = p_z \Delta p + \frac{(\Delta p)^2}{2}, \qquad (11)$$

where $p_z \propto 1/n$ is the $z$ component of electron momentum immediately before the kick. The energy change due to the offset field during the first half of the period prior to the kick

$$\Delta E^{\rm offset}_{(1)} \simeq -\Delta z F_{\rm offset} \simeq -p_z \frac{T_T}{2} F_{\rm offset} \qquad (12)$$

while during the second half after the kick

$$\Delta E^{\rm offset}_{(2)} \simeq -(p_z+\Delta p)\frac{T_T}{2} F_{\rm offset}. \qquad (13)$$

The energy transfer during one period due to the offset field is thus

$$\Delta E^{\rm offset} = \Delta E^{\rm offset}_{(1)} + \Delta E^{\rm offset}_{(2)} \simeq -\left(p_z + \frac{\Delta p}{2}\right) T_T F_{\rm offset}. \qquad (14)$$

The resulting total energy transfer during one period

$$\begin{aligned} \Delta E &= \Delta E^{\rm kick} + \Delta E^{\rm offset} \\ &= \left(p_z + \frac{\Delta p}{2}\right)(\Delta p - T_T F_{\rm offset}) \\ &= -\left(p_z + \frac{\Delta p}{2}\right) T_T F_{\rm av}. \end{aligned} \qquad (15)$$

As expected when $F_{\rm av} = F_{\rm offset} - \Delta p/T_T = 0$, the energy transfer vanishes. Note that Eq. (15) is only valid to first order in $T_T$ when the linear approximation $\Delta z = p_z T_T/2$ in Eqs. (12) and (13) holds. This approximation is valid in the high-frequency limit $T_T \ll T_n$ and for local momenta $p_z$ of the order of the mean orbital momentum $\langle p_z \rangle \simeq 1/n \ll \Delta p$. It breaks down near the nucleus. Consequently, the electron gains or loses energy every time it is scattered at the nucleus. It is this residual random net energy transfer that renders the electron dynamics chaotic near threshold (see Fig. 1). However, given that the orbital periods of very-high-$n$ states are long, the electron spends much of its time well removed from the nucleus where it behaves essentially as a quasifree particle which allows the atom to survive a large number of HCPs and undergo transient stabilization. When the balance between the impulses provided by the HCPs and offset field is broken, i.e., when $F_{\rm av} \neq 0$, the energy transfer becomes nonzero resulting in the marked decreases in survival probability evident in Figs. 2 and 4. Closer inspection of these data reveals that, especially for high scaled frequencies, the maximum in survival probability does not occur precisely at $F_{\rm av} = 0$, and that the peak in the survival probability is asymmetric. This results because symmetry is broken by the quasi-1D initial state. If, for example, $F_{\rm av} > 0$ the electron must escape the atom in the $-z$ direction. Thus if the atom is initially oriented along the $+z$ axis the electron must transit to the other side of the nucleus before ionization can occur, which takes time. The same need does not exist if the atom is initially oriented along the $-z$ axis. [No similar asymmetry is observed using (unpolarized) K(351$p$) atoms [19].]

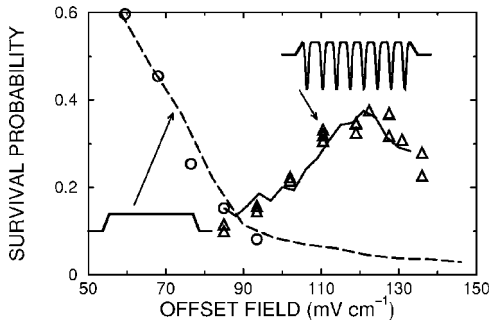


FIG. 5. Survival probability for K(351$p$) atoms as a function of offset field $F_{\rm av}$. The open circles show experimental results, and the dashed line CTMC simulations, with only $F_{\rm offset}$ present. The open triangles and solid line show results obtained when a train of HCPs delivering scaled impulses $\Delta p_0 = 0.73$ with scaled frequency $\nu_0 = 3.3$ is superposed on $F_{\rm offset}$. The simulations assume ±5% noise and $n_{\rm max} = 1000$ (see text).

## V. STRONG KICKS: FRUSTRATED FIELD IONIZATION

The threshold field for classical ionization of the downhill Stark state $[E_{\rm Stark} = H_{\rm at} + zF \sim -1/(2n^2) - (3/2)n^2 F]$ is

$$F_c = \frac{1}{9n^4} \qquad (16)$$

or $F_{c,0} = 1/9$. Thus the presence of offset fields larger than this value will lead to direct field ionization when no HCPs are applied. Such ionization, however, is suppressed by the presence of an (oppositely directed) HCP train giving rise to "pulse-frustrated field ionization" in which the HCPs counteract static field ionization by periodically driving the escaping electron back to the nucleus. Under these conditions the presence of the HCP train results in an increase in the overall survival probability. This effect should be observed with any initial state irrespective of its polarization. It is illustrated in Fig. 5 which shows survival probabilities for K(351$p$) atoms as a function of $F_{\rm offset}$ with and without HCPs present. The data refer to $N = 20$ HCPs with a scaled frequency $\nu_0 = 3.3$ and scaled strength $\Delta p_0 = 0.73$. The CTMC simulations assume that product states with $n \gtrsim n_{\rm max} = 1000$ are ionized and include 5% period and amplitude noise on the HCP train. The theoretical predictions are in good agreement with the experimental results. In the absence of HCPs, more than 90% of the parent atoms are ionized in offset fields of

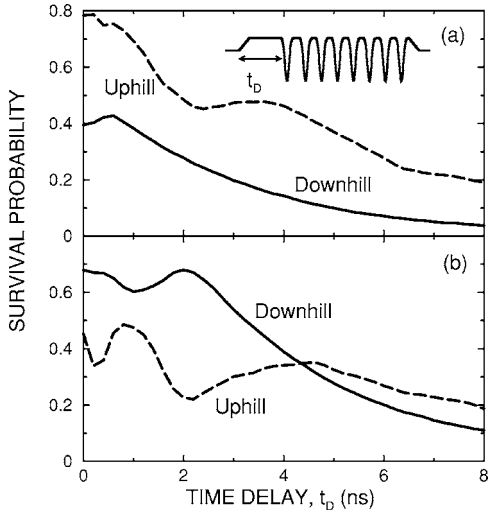


FIG. 6. Survival probability for quasi-1D $n_i=350$ Rydberg atoms as a function of the time delay $t_D$ between the rise of the offset field and the beginning of the HCP train. The train delivers scaled impulses $\Delta p_0=0.73$ with scaled frequency $\nu_0=3.3$. The simulations assume ±5% noise. The offset field is set to (a) $F_{\text{offset}}=\Delta p \nu_T$, i.e., $F_{\text{av}}=0$, and (b) $F_{\text{offset}}=120$ mV/cm, i.e., $F_{\text{av},0}=n_i^4 F_{\text{av}}=-0.027$ a.u.

100 mV cm$^{-1}$. Application of the HCP train leads to a dramatic increase in survival probability, reaching a maximum of ~40% for an offset field of ~120 mV cm$^{-1}$ which corresponds to an average field $F_{\text{av}}\sim 0$. This observation indicates that pulse-frustrated field ionization is a direct consequence of the same transient stabilization mechanism discussed earlier.

While pulse-frustrated field ionization is expected to occur for any initial state, its effectiveness will depend markedly on its polarization. This is due to the fact that field ionization of quasi-1D Rydberg atoms is quite sensitive to their orientation [20,23]. A similar sensitivity to the polarization of Rydberg atoms has also been observed in ion-atom collisions [24]. In a given applied field states oriented towards the saddle point, termed "downhill" states, ionize at much earlier times than "uphill" states oriented in the opposite direction. While electrons in downhill states can cross the saddle point directly, those in uphill states must precess to the downhill side before ionization. The dynamics of the electron therefore is quite different depending on which side of the nucleus it is initially located. This sensitivity has been used to measure the polarization of quasi-1D states as well as the dynamics of field ionization [20,23]. Here we suggest that pulse-frustrated field ionization might also be used to probe atomic polarization. To demonstrate this, Fig. 6 shows calculated survival probabilities for the present combinations of quasi-1D uphill and quasi-1D downhill states as a function of the time delay $t_D$ between the rise of the offset field and the beginning of the HCP train (see inset). The offset field is turned off after the last HCP. Thus the offset field pulse is longer than the HCP train. For the results in Fig. 6(a), the size of the offset field and the HCPs is set such that $F_{\text{offset}}=-\Delta p/T_T$, i.e., $F_{\text{av}}=0$ during the HCP train. The simulations assume a train of $N=20$ HCPs of scaled strength $\Delta p_0=0.73$ and scaled frequency $\nu_0=3.3$, and again include 5% noise in the HCP train.

The downhill initial state is quite unstable because much of its electron probability density is located near or beyond the saddle point. The survival probability decreases rapidly as the delay time $t_D$ increases and the electrons travel further from the saddle point before the HCP train begins. A small increase in survival probability is observed at early times and is associated with the portion of the initial wave packet (or subensemble of classical trajectories) initially moving towards the nucleus. The uphill state, which is initially localized on the other side of the nucleus, is significantly more stable. The oscillatory structure seen in the survival probability provides direct information on the motion of the electron in the offset field. Prior to application of the offset field the electron probability density is greatest near the outer classical turning point, located at $z<0$, and the electron has a binding energy $H_{\text{at}}(0)=E_i$. After a delay time $t_D$ the energy becomes

$$E(t_D) = E_i - F_{\text{offset}}[z(t_D) - z(0)], \tag{17}$$

where the second term in this equation is the work done by the offset field on the electron. Between the time the offset field is switched on and the time the electron reaches the nucleus, the work done by the field is positive and the electron continuously gains energy, consequently decreasing the survival probability. Conversely, after the electron is scattered at the nucleus and before it again reaches the outer turning point, the work done by the offset field is negative and, therefore, the electron continuously loses energy and the survival probability increases. Application of the HCP train counteracts the effect of the offset field and tends to suppress further ionization. The overall survival probability therefore provides direct information on the electron dynamics in the offset field during the period up to $t_D$.

The sensitivity to the initial atomic polarization can be enhanced by arranging the sizes of the offset field and HCPs such that $F_{\text{av}}$ is small and negative [Fig. 6(b)]. Before application of the HCP train the saddle point due to $F_{\text{offset}}(>0)$ is located at $z<0$ and electrons leave their parent atoms traveling in the $-z$ direction. In contrast, with the HCPs applied, the saddle point associated with the net average field $F_{\text{av}}(<0)$ is located at $z>0$. Consequently the electron must leave in the $+z$ direction. The stability of uphill and downhill states is interchanged and both uphill and downhill states exhibit oscillatory behavior as the delay time $t_D$ is varied. In particular, electrons in the downhill state, after initially traveling towards the saddle point associated with the offset field must turn around to exit in the opposite direction, their final energy gain/loss depending on their phase space coordinates when the HCPs are turned on. In fact, the oscillation in the survival probability reflects the precession of the downhill states relative to the offset field which have now become uphill states with respect to the net average field. Thus, the stability of a quasi-1D initial state is critically dependent on any slight mismatch between the offset field and the HCP train, i.e., on $F_{\text{av}}$.

## VI. CONCLUSION

The dynamics of Rydberg atoms subject to a train of HCPs in the presence of a superposed offset field have been investigated. The phase-space portraits show a clear sensitivity to the polarization of the initial wave function due to the existence of quasistable islands (cantori) on only one side of the nucleus. In practice, however, such quasiregular structures do not play an important role in the dynamics because most of the Rydberg atom population quickly becomes traped close to the ionization threshold, which is immersed in the chaotic sea. The transient stabilization of these extremely high-$n$ states is essentially independent of the initial atomic polarization and is governed by the average field $F_{\mathrm{av}}=F_{\mathrm{offset}}-\Delta p/T_T$, being strongly enhanced when $F_{\mathrm{av}}=0$. Since the dynamics occur in the chaotic sea, it is robust against noise in the HCP train. When the offset field is much larger than the classical field ionization threshold, application of a train of HCPs can frustrate the field ionization process and suppress ionization. By introducing a time delay between application of the offset field and initiation of the HCP train, the survival probability becomes sensitive to the polarization of the initial wave function, especially when the net average field is slightly different from zero. Such sensitivity can be used to probe the polarization of wave functions. A quantum analysis of the transient stabilization phenomenon studied here is of interest but difficult to accomplish because of the extremely-high-$n$ states involved. Quantum mechanically, the transient stabilization in high-$n$ states might be even more robust than predicted by classical simulations [20,22].

## ACKNOWLEDGMENTS

This research is supported by the Grant Nos. FWF-SFB-F016 and FWF-P15025 (Austria), OBES, the U.S. DOE to ORNL managed by the UT-Batelle LLC under Contract No. DE-AC05-00OR22725, the NSF (Grant No. PHY-0353424), and the Robert A. Welch Foundation. J. C. Lancaster acknowledges support from the ONR.

[1] G. Casati, B. V. Chirikov, F. M. Izraelev, and J. Ford, *Lecture Notes in Physics* (Springer, New York, 1979).
[2] G. Casati, B. V. Chirikov, D. L. Shepelyansky, and I. Guarneri, Phys. Rep. **154**, 77 (1987).
[3] R. V. Jensen, S. M. Susskind, and M. M. Sanders, Phys. Rep. **201**, 1 (1991).
[4] A. Buchleitner, D. Delande, and J. Zakrzewski, Phys. Rep. **368**, 409 (2002).
[5] A. Buchleitner and D. Delande, Phys. Rev. Lett. **75**, 1487 (1995).
[6] F. B. Dunning, J. C. Lancaster, C. O. Reinhold, S. Yoshida, and J. Burgdörfer, Adv. At., Mol., Opt. Phys. **52**, 49 (2005).
[7] M. Kalinski and J. H. Eberly, Opt. Express **1**, 216 (1997).
[8] C. O. Reinhold, S. Yoshida, J. Burgdörfer, B. E. Tannian, C. L. Stokely, and F. B. Dunning, J. Phys. B **34**, L551 (2001).
[9] H. Maeda, D. V. L. Norum, and T. F. Gallagher, Science **307**, 1757 (2005).
[10] S. Yoshida, C. O. Reinhold, E. Persson, J. Burgdörfer, and F. B. Dunning, J. Phys. B **38**, S209 (2005).
[11] M. T. Frey, F. B. Dunning, C. O. Reinhold, S. Yoshida, and J. Burgdörfer, Phys. Rev. A **59**, 1434 (1999).
[12] B. E. Tannian, C. L. Stokely, F. B. Dunning, C. O. Reinhold, S. Yoshida, and J. Burgdörfer, Phys. Rev. A **62**, 043402 (2000).
[13] D. You, R. R. Jones, P. H. Bucksbaum, and D. R. Dykaar, Opt. Lett. **18**, 290 (1993).
[14] N. E. Tielking and R. R. Jones, Phys. Rev. A **52**, 1371 (1995).
[15] J. Bromage and C. R. Stroud, Phys. Rev. Lett. **83**, 4963 (1999).
[16] A. Wetzels, A. Gurtler, L. D. Noordam, F. Robicheaux, C. Dinu, H. G. Muller, M. J. J. Vrakking, and W. J. van der Zande, Phys. Rev. Lett. **89**, 273003 (2002).
[17] E. Persson, S. Puschkarski, X. M. Tong, and J. Burgdörfer, in *Ultrafast Optics, Springer Series in Optical Sciences*, edited by F. Krausz, G. Korn, P. Corkum, and I.. A. Walmsley (Springer, Berlin, 2004).
[18] C. Wesdorp, F. Robicheaux, and L. D. Noordam, Phys. Rev. Lett. **87**, 083001 (2001).
[19] W. Zhao, J. C. Lancaster, F. B. Dunning, C. O. Reinhold, and J. Burgdörfer, J. Phys. B **38**, S191 (2005).
[20] C. L. Stokely, J. C. Lancaster, F. B. Dunning, D. G. Arbó, C. O. Reinhold, and J. Burgdörfer, Phys. Rev. A **67**, 013403 (2003).
[21] C. F. Hillermeier, R. Blümel, and U. Smilansky, Phys. Rev. A **45**, 3486 (1992).
[22] G. Casati, I. Guarneri, and G. Mantica, Phys. Rev. A **50**, 5018 (1994).
[23] C. O. Reinhold, J. Burgdörfer, R. R. Jones, C. Raman, and P. H. Bucksbaum, J. Phys. B **28**, L457 (1995).
[24] D. M. Homan, O. P. Makarov, O. P. Sorokina, K. B. MacAdam, M. F. V. Lundsgaard, C. D. Lin, and N. Toshima, Phys. Rev. A **58**, 4565 (1998).